

Article

Using Manganese Oxidizing Fungi to Recover Metals from Electronic Waste

Sarah A. Doydora ¹, Oliver Baars ^{2,3} , Marc A. Cubeta ^{2,3} and Owen W. Duckworth ^{1,2,*} ¹ Department of Crop and Soil Sciences, North Carolina State University, Raleigh, NC 27695, USA² Center for Integrated Fungal Research, North Carolina State University, Raleigh, NC 27695, USA; obaars@ncsu.edu (O.B.); macubeta@ncsu.edu (M.A.C.)³ Department of Entomology and Plant Pathology, North Carolina State University, Raleigh, NC 27695, USA

* Correspondence: owen_duckworth@ncsu.edu; Tel.: +1-919-513-1577

Abstract: Discarded electronic materials (e-waste) contain economically valuable metals that can be hazardous to people and the environment. Current e-waste recycling approaches involve either energy-intensive smelting or bioleaching processes that capture metals in their dissolved forms. Our study aimed to use Mn oxidizing fungi for recovering metals from e-waste that could potentially transform recycled metals directly into solid forms. We hypothesized that Mn oxidizing fungi can extract metals through chelation by siderophores and subsequent metal (or metal-chelate) adsorption to Mn oxides produced by fungi. Pure cultures of the three fungal species examined were grown on solidified Leptothrix medium with or without ground lithium ion batteries and incubated under ambient room temperature. The results showed Mn and Co were recovered at the highest concentrations of 8.45% and 1.75%, respectively, when grown with *Paraconiothyrium brasiliensis*, whereas the greatest concentration of Cu was extracted by *Paraphaeosphaeria sporulosa* at 20.6% per weight of e-waste-derived metals. Although metal-siderophore complexes were detected in the fungal growth medium, metal speciation data suggested that these complexes only occurred with Fe. This observation suggests that reactions other than complexation with siderophores likely solubilized e-waste metals. Elemental mapping, particularly of *P. brasiliensis* structures, showed a close association between Mn and Co, suggesting potential adsorption or (co)precipitation of these two metals near fungal mycelium. These findings provide experimental evidence for the potential use of Mn oxidizing fungi in recycling and transforming e-waste metals into solid biominerals. However, optimizing fungal growth conditions with e-waste is needed to improve the efficiency of metal recovery.

Keywords: e-waste; Mn oxidizing fungi; siderophores; metals

Citation: Doydora, S.A.; Baars, O.; Cubeta, M.A.; Duckworth, O.W. Using Manganese Oxidizing Fungi to Recover Metals from Electronic Waste. *Minerals* **2024**, *14*, 111. <https://doi.org/10.3390/min14010111>

Academic Editors: María Sofía Urbieto and Laura Castro

Received: 7 December 2023

Revised: 10 January 2024

Accepted: 18 January 2024

Published: 20 January 2024



Copyright: © 2024 by the authors. Licensee MDPI, Basel, Switzerland. This article is an open access article distributed under the terms and conditions of the Creative Commons Attribution (CC BY) license (<https://creativecommons.org/licenses/by/4.0/>).

1. Introduction

Globally, discarded electronic materials, or e-waste, are generated at approximately 50 million tonnes per year [1], with USA production reported at 6.92 metric tonnes in 2019 [2]. E-waste presents a largely untapped resource for valuable materials, including valuable transition metals and rare earth elements [3]. However, of all the e-waste generated globally, less than 13% is recycled, with the bulk landfilled, incinerated, or exported to other countries [4]. Owing to its highly variable and potentially toxic contents, the recycling of e-waste involves intensive manual sorting and ultimately energy-intensive smelting. These processes can pose a major hazard to occupational safety and the environment. To better protect human health and the environment and conserve the use of metal resources, novel microorganism-based strategies for recycling e-wastes are needed [5,6].

The use of microorganisms or biomolecules to solubilize metals from e-waste, known as bioleaching, has garnered attention as a potential alternative to conventional recycling processes [7,8]. Because of the simplicity and lower energy requirements, the bioleaching of e-waste is considered a promising sustainable technology [9]. However, the end product of this technique may require further processing to produce the more desirable

solidified form of reclaimed metals. Given an established market for solid metals, there is a need for microorganism-based approaches capable of transforming solubilized metals into concentrated solids.

Fungi are widely used in technological applications and have been identified as key players in developing circular economies [10]. Moreover, Mn oxidizing fungi are known to exude organic complexing agents, which are capable of binding certain metals (known as siderophores [11–14]) and are also known to produce Mn biominerals. Naturally produced Mn oxides, such as birnessite, are strong metal sorbents [15] and are referred to as the “scavenger of the sea”, owing to their high sequestering capacity for metals in marine water [16]. In the same manner, fungal Mn biominerals may retain siderophore-bound metals [17], including those solubilized from e-waste metals. However, currently, the effect of siderophores and manganese oxide production on the bioleaching process and the ultimate fate of recovered metals is largely unknown. This study aimed to determine the ability of Mn oxidizing fungi to grow on e-waste, mobilize its useful metals, and produce Mn biominerals to capture e-waste metals in an easily reusable form.

2. Materials and Methods

2.1. E-Waste

A sample of ground Li ion batteries provided by Retrie Technologies (Lancaster, OH, USA) was used as received. The metal contents of the ground e-waste are shown in Figure 1.

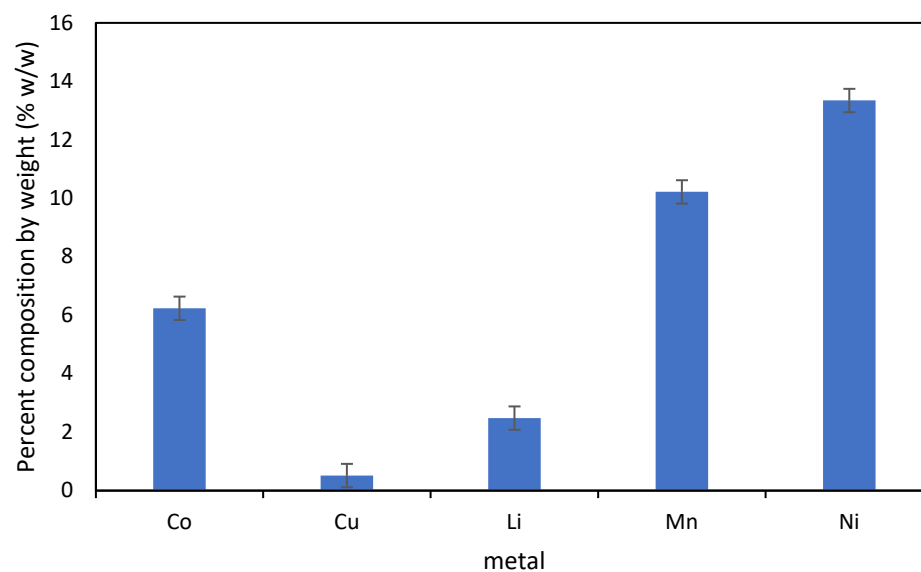


Figure 1. Metal contents in the ground Lithium (Li) battery residues.

2.2. Fungal Cultures

Manganese oxidizing fungi were isolated from NC State’s Lot 86 superfund site, and identified by microscopic morphology and ITS rDNA sequence analysis [18]. At this site, unwanted biogenic birnessite had precipitated from the oxidation of dissolved Mn(II) present in the groundwater of the site. The birnessite deposited in the treatment system also effectively adsorbed several metals, including Cu, Zn, Co, Ni [19,20].

We selected fungal cultures for experiments because these fungi oxidized manganese that could sorb metals and were presumably tolerant to potentially toxic metals based on the location of isolation. Pure cultures of three fungal cultures—*Paraconiothyrium brasiliensis* (accession number PP101868), *Phoma herbarium* (accession number PP101869), and *Paraphaeosphaeria sporulosa* (accession number PP101870) [21]—were regenerated from frozen cultures (kept under $-80\text{ }^{\circ}\text{C}$). The isolates were cultured at room temperature on Petri dishes containing solidified Leptothrix medium [22], which was chosen because it

has been used previously to grow these and related fungi such that they produce Mn oxides [19,21] and does not interfere with the chrome azurol S (CAS) assay [23,24]. The fungi were transferred two consecutive times between 7 and 14 d of incubation [19,21,23,24]. After which, the second fungal cultures were stored at 4 °C and used as the fungal sources for the incubation and extraction experiments. In preliminary experiments, these isolates were determined to produce both manganese oxides and siderophores in the presence of the e-waste, evaluated visually by using the layer plate chrome azurol S (CAS) assay [23].

2.3. Incubation Experiment and Extractions

The fungal isolates were tested for metal recovery from the ground Li ion battery e-waste. Four replicates of the selected isolates were grown on top of Whatman No. 1 filter paper on a solidified Leptothrix medium [22] with (1 g e-waste L⁻¹ culture medium) or without the ground battery. After 2 weeks of room temperature incubation (23–25 °C), filter papers from the three replicates were removed from the underlying agar plate. Metal recovery from the fungal mycelium on the filter papers was obtained through total digestion and metal analysis of digestate for each of the three replicates via inductively coupled plasma optical emission spectroscopy (Perkin Elmer 8000 inductively-coupled plasma-optical emission spectrometer, Waltham, MA, USA; ICP-OES) at the Environmental and Agricultural Testing Service Laboratory (EATS, NC State University, Raleigh, NC, USA).

The fourth plate from each culture (with or without e-waste) was harvested by splitting the residual medium into two equal halves. One half of the medium was extracted two times sequentially with 20 mL of 100% methanol followed by 30 min sonication and centrifugation. The supernatants from the two sequential extractions were combined in 50 mL Falcon tubes for metal speciation by liquid chromatography–inductively coupled plasma-mass spectrometry (Section 2.4). The other half was extracted similarly using 0.1% formic acid in methanol for siderophore analysis by colorimetric assays and liquid chromatography-electrospray ionization-mass spectrometry (Section 2.5).

2.4. Analysis of Metal Speciation by Liquid Chromatography–Inductively Coupled Plasma-Mass Spectrometry (LC-ICP-MS)

Agar gel extracts in 100% methanol were syringe-filtered (0.2 µm) and directly analyzed by liquid chromatography–inductively coupled plasma-mass spectrometry (LC-ICP-MS) without additional sample preparation. The LC-ICP-MS platform consisted of a liquid chromatography system (Ultimate 3000, ThermoFisher, Waltham, MA, USA) coupled to an ICP-MS (iCAP RQ, ThermoFisher, Waltham, MA, USA). Reversed phase chromatography was performed with a C18 column (ACE Excel 1.7 SuperC18, 2.1 × 100 mm). The injected samples (25 µL) were separated at pH = 6.5 under a gradient of solutions A and B (solution A: water, 5 mM ammonium acetate, pH 7; solution B: methanol, 5 mM ammonium acetate; gradient 2%–100% B, flow rate 0.4 mL min⁻¹). The column outflow was split using a flow splitter (Analytical Scientific Instruments, 600-PO10-06, Richmond, CA, USA) to introduce 0.1 mL min⁻¹ into the ICP-MS with a zero dead volume PFA micro nebulizer (Elemental Scientific, Omaha, NE, USA). Oxygen was used as an added gas in the ICP-MS (flow 8.75 mL min⁻¹) to minimize carbon deposition on the ICP-MS cones (Pt cones) at high organic buffer concentrations. The instrument was operated in KED mode with He as a collision gas to analyze element signals including ⁵⁵Mn, ⁵⁶Fe, ⁵⁹Co, and ⁶³Cu. Concentrations of siderophores were calculated using peak areas of eluting iron peaks and external standards of the ferric chelate of the siderophore ferrioxamine B (10–100 µM).

2.5. Siderophore Analysis by Colorimetric Assays and Liquid Chromatography–Electrospray Ionization-Mass Spectrometry (LC-ESI-MS)

The Agar gel extracts for LC_ESI_MS (0.1% formic acid in 100% methanol) were evaporated to dryness in a SpeedVac (ThermoFisher, Waltham, MA, USA), and reconstituted in 0.5 mL of methanol and 3.5 mL of high-purity water (18 MΩ, MQ). The reconstituted samples were acidified with 0.1% formic acid and passed over reversed-phase solid-phase extraction (SPE) cartridges (Oasis HLB, 400 mg). The cartridges were washed with 2 mL

of 0.1% formic acid and eluted once with 2 mL of 30% methanol and twice with 2 mL of 80% methanol. The three eluate fractions were pooled and diluted 1:1 with water for analysis with two assays: the CAS assay to quantify unbound siderophores [25] and the Arnou assay to quantify catechol siderophores [26].

Siderophore analysis by liquid chromatography–electrospray ionization–mass spectrometry (LC-ESI-MS) followed previously reported methods [27,28]. A volume of 100 µL of the extract (see above) was diluted 1:2 with water. A mass unit resolution single quadrupole LC-MS (ISQ-EC, ThermoFisher, Waltham, MA, USA) which was coupled with an ultraviolet–visible (UV-vis) spectrophotometer and a charged aerosol detector (ThermoFisher, Waltham, MA, USA). A sample volume of 25 µL was injected and separated under a gradient of solvents A and B (unless otherwise noted A: water, 0.1% formic acid, 1% acetonitrile; B: acetonitrile, 0.1% formic acid, 2% water; gradient: 0–1.5 min 0% B, 1.5–8 min 0%–100% B; 8–10 min 100% B; re-equilibration at 100% A for 4 min). Separation was accomplished with an Agilent Poroshell 120 EC-C18 column (4.6 × 100 mm, 2.7 µm) and a flow rate of 1.2 mL/min and the column temperature was 30 °C. Additionally, to acquire high-resolution MS and MS/MS data to enable siderophore identification, the selected samples were additionally analyzed with a high-resolution LC-MS/MS platform (Orbitrap Exploris 480, ThermoFisher). Sample volumes of 25 µL were injected and separated using a Restek Raptor C18 (2.1 × 100) column with a flow rate of 0.4 mL/min and the column compartment was kept at 45 °C. The LC gradient was identical to that used with the ISQ-EC described above. Full-scan mass spectra ($m/z = 85\text{--}1200$) were acquired in positive ionization mode with the resolution set to $R = 60,000$ (full width at half maximum at $m/z = 400$) and data-dependent MS/MS acquisition of the top 5 most abundant ions in each cycle. Product ions were generated in HCD mode with 35 eV collision energy and an isolation window of 1.5 Da. The resolving power for MS/MS analysis was $R = 15,000$ (full width at half maximum at $m/z = 400$). Prior to injection, samples were syringe filtered (0.2 µm, PES membrane) and 150 µM of FeCl₃ (addition of 3 µL of a 5 mM FeCl₃ stock) was added to produce iron–siderophore complexes to screen siderophore by utilizing the natural ⁵⁴Fe–⁵⁶Fe stable iron isotope pattern [27]. There was no visible color change after the addition of FeCl₃ to the extracts.

2.6. Scanning Electron Microscopy with Energy Dispersive X-ray Spectrometry

To evaluate the morphology and elemental distribution on the fungal mycelium, portions of intact cultures of unextracted replicates for each of the fungal isolates grown with e-waste were analyzed using a Hitachi SU8700 scanning electron microscope (Hitachi High-Tech, Tokyo, Japan) equipped with an Oxford Ultimex 65 energy dispersive X-ray spectrometer (SEM-EDS) (Oxford Instruments NanoAnalysis, High Wycombe, Buckinghamshire, UK). Fibrous samples were secured to SEM stubs using double-sided carbon tape. The thickness of the sample was sufficient to prevent any contribution from the carbon tape background affecting the results. The SEM was operated with a 20 keV high probe current beam under variable pressure conditions (70 Pa dry N₂ backfill) to prevent charging [29]. The probe current was not measured directly and was set to optimize X-ray data collection.

3. Results

Fungal recovery of metals in solids associated with vegetative mycelium from the ground e-waste varied among the three species (Figure 2). *P. brasiliensis* recovered the most Mn (at 8.45%) and Co (at 1.75%), followed by *P. herbarium* at (2.06% Mn and 0.76% Co) and *P. sporulosa* (0.15% each for Mn and Co). In contrast, *P. sporulosa* recovered the most Cu at 20.59%, followed by *P. brasiliensis* at 5.24% and *P. herbarium* at 3.07%. The percentage of Ni recovered by all fungal species was small (0.33%–0.45%).

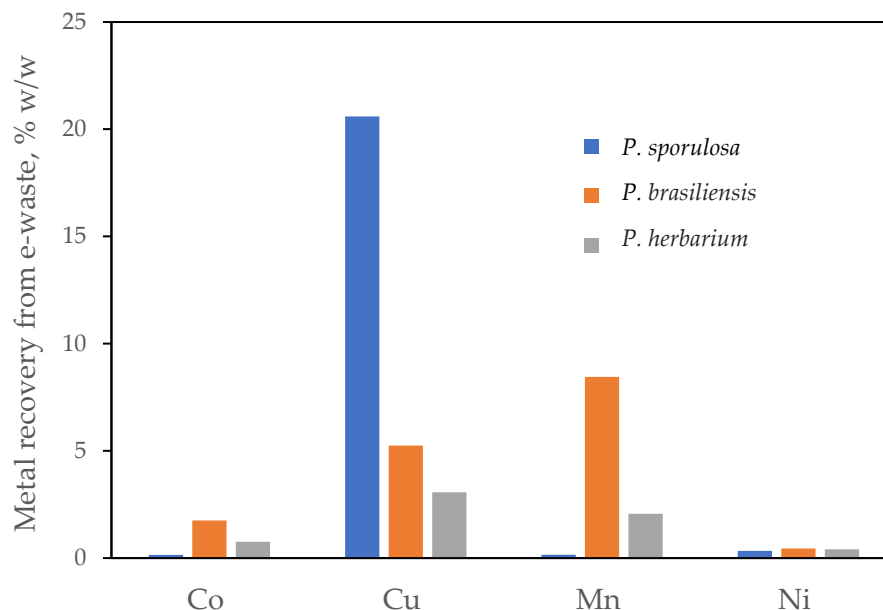


Figure 2. Percent recovery of metals from e-waste by *Paraconiothyrium brasiliensis* (orange), *Paraphaeosphaeria sporulos* (blue), and *Phoma herbarium* (gray) cultured in solidified Leptothrix medium.

Images obtained from scanning electron microscopy (SEM) with energy dispersive spectroscopy (EDS) show the close association between the Mn and Co hotspots in areas where a network of fungal mycelium was highly concentrated, particularly for *P. brasiliensis* rather than for *P. sporulosa* (Figure 3). In contrast, Cu and Ni were not observed in SEM-EDS spectra samples of mycelium from both species, whereas none of these metals were detected on mycelial samples from *P. herbarium*, which is consistent with its generally low recoveries.

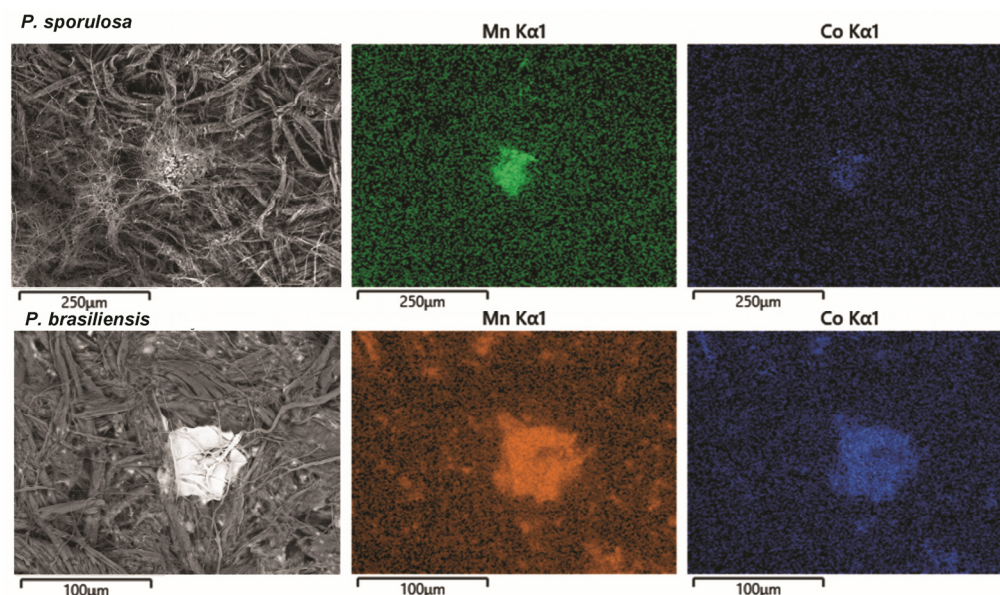


Figure 3. Scanning electron microscope image and elemental maps (Mn and Co) of *Paraconiothyrium brasiliensis* and *Paraphaeosphaeria sporulos*.

The speciation of metals recovered from the extracted medium is shown in Figure 4. Based on the LC-ICP-MS results, Mn, Co, and Cu in the three fungal extracts eluted early (retention time (RT) < 2 min), similar to the metals extracted from the sterile controls (viz., plates with no fungi; Figure 4A–C). These results suggest that the recovered metals occurred largely in their inorganic forms in the fungal mycelium. In contrast, although not a major component of the e-waste, Fe in the culture medium had a small peak early in the

chromatogram (RT < 2 min), but also showed peaks at longer retention times (RT > 5 min) in all samples grown with fungi (Figure 4D), which had retention times more similar to Fe(III)-DFOB standards. These peaks suggest that Fe was selectively bound in all fungal extracts, except in the fungi-free controls, with a larger fraction of Fe bound in the presence of e-waste, as demonstrated by the larger peaks at RT > 5 in Figure 4D.

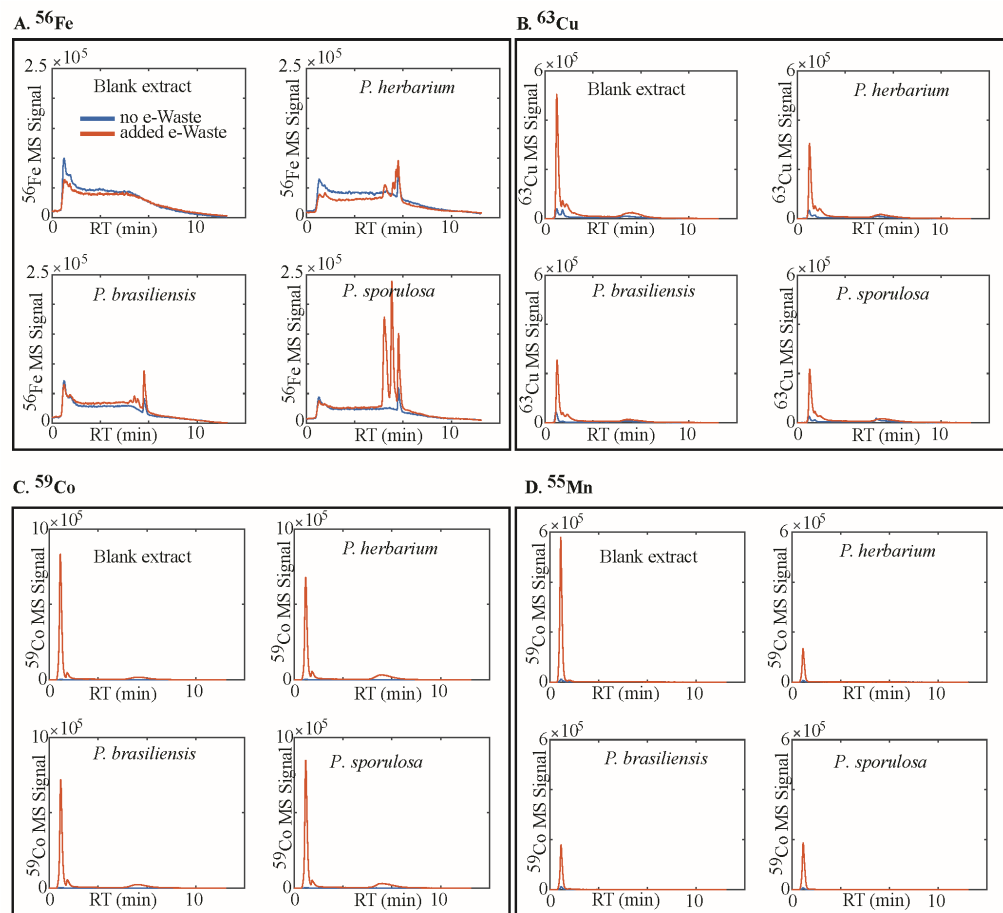


Figure 4. Metal speciation of (A) Fe, (B) Cu, (C) Co, and (D) Mn extracted from the biomass-free residual fungal culture medium after 14 d of incubation at room temperature and analyzed using LC-ICP-MS.

Information about the structure of Fe complexes in medium extracts was obtained by LC-ESI-MS (Figure 4). Fungal Fe complexes with a RT of ~6.3 min were identified as the siderophore ferricrocin based on high-resolution mass matches in MS and MS/MS (Table 1, Figure 5). The ferricrocin complex had a mass of 771.2478, which matched the expected mass of the iron–ferricrocin complex ($[M+H]^+ = C_{28}H_{45}N_9O_{13}Fe$, expected $m/z = 771.2481$, $\Delta m/z = 0.4$ ppm) [30,31] and showed the characteristic ^{54}Fe - ^{56}Fe isotope pattern. The MS/MS fragmentation was in agreement with a published MS/MS spectrum a(GNPS CCMSLIB00005436133) [32]. The iron free form of ferricrocin was not detected ($m/z = 718.3367$). Although ferricrocin complexes were detected in all fungal extracts with or without e-waste, concentrations were up to three times greater in the presence of e-waste (Table 2). In addition to iron ferricrocin, several Fe complexes were observed in fungal extracts in the presence of e-waste (RT ~5–6.3 min) (Figure 5). The MS and MS/MS spectra were in agreement with different coprogen-type siderophores (dimethylcoprogen, 2-N-methylcoprogen B, and 2-N-methylcoprogen B with an additional oxygen group). The MS/MS fragmentation of all of the coprogen-type siderophores showed $m/z = 538.171$ as the most abundant fragment, which matched the substructure dimerum acid that is formed during coprogen fragmentation [33].

Table 1. Siderophores detected in culture agar extracts.

#	<i>m/z</i> exp.	<i>m/z</i> calc.	Δ ppm	Formula	RT (min)	Identity	MS/MS Fragments (Intensity)	Reference
1	771.2478	771.2481	0.4	C ₂₈ H ₄₅ O ₁₃ N ₉ Fe	6.4	Ferricrocin	398.088 (100); 455.110 (85); 581.15 (74); 599.164 (73); 370.098 (63); 553.157 (45)	GNPS Library Spectrum CCM- SLIB00005436133 [30–32]
2	808.3295	808.33	0.6	C ₃₅ H ₅₅ O ₁₂ N ₆ Fe	7.9	coprogen-type (dimethylcoprogen)	538.171 (100)	[33]
3	810.3087	810.3098	1.4	C ₃₄ H ₅₄ O ₁₃ N ₆ Fe	5.4	coprogen-type (hydroxy-2-N- methylcoprogen)	538.171 (100)	[33]
4	794.3139	794.3144	0.6	C ₃₄ H ₅₄ O ₁₂ N ₆ Fe	5.9	coprogen-type (2-N- methylcoprogen)	538.171 (100)	[33]

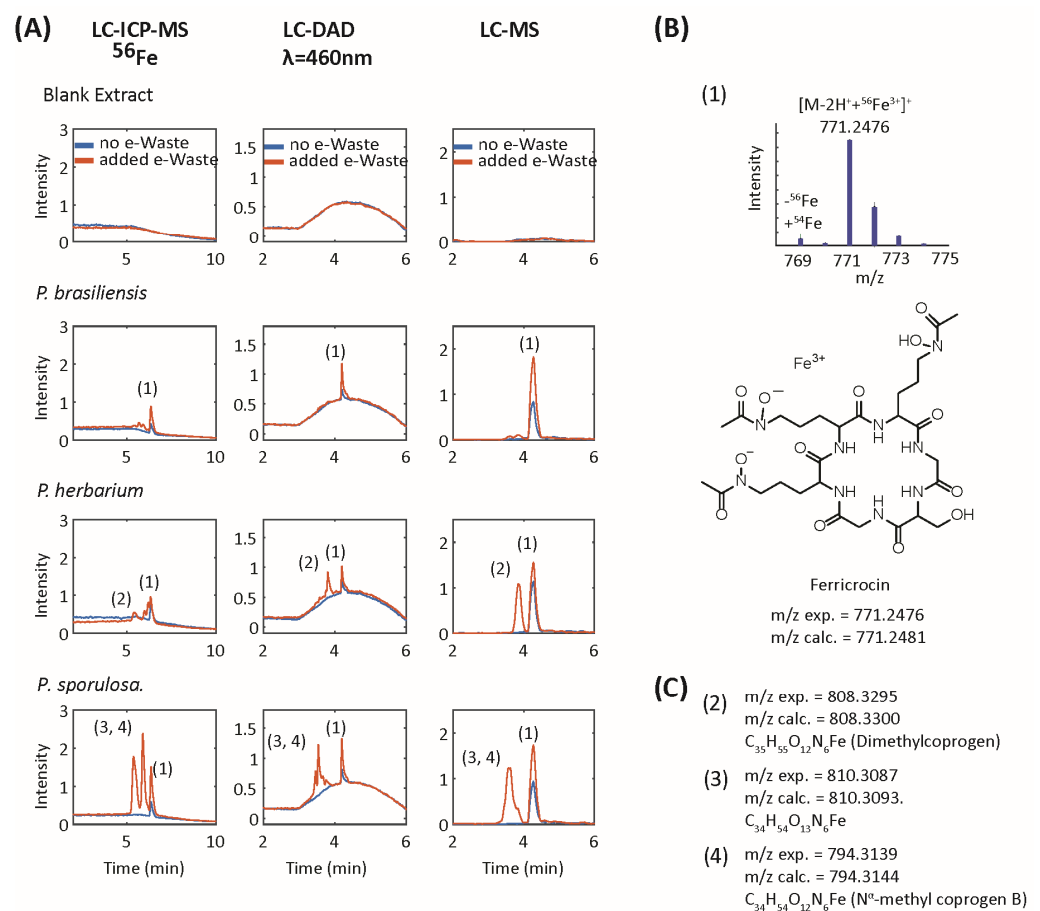


Figure 5. Iron–siderophore complexes in culture medium with (red trace) and without (blue trace) e-waste. **(A)** Chromatograms of the LC-ICP-MS experiment, LC-diode array detector data at 460nm and LC-ESI-MS extracted ion chromatograms of the major detected siderophores. **(B)** ⁵⁴Fe–⁵⁶Fe isotope pattern used to screen for iron–siderophore complexes in the LC-ESI-MS data, through the example of the siderophore ferricrocin, as produced by all cultures. Ferricrocin was identified by a match of MS/MS data with published MS/MS data (see Table 1). **(C)** Coprogen-type siderophores detected in the culture media of *P. herbarium* and *P. sporulosa* based on analysis of the MS/MS spectra (see text).

Table 2. Concentrations of siderophores detected and measured in the culture agar extracts.

Culture	Siderophore	Concentration (μM)
<i>P. sporulosa</i> + e-waste	3	67.5
	4	60.4
	1	31.9
<i>P. sporulosa</i> – e-waste	1	10.8
<i>P. brasiliensis</i> + e-waste	1	18.2
<i>P. brasiliensis</i> – e-waste	1	7.1
<i>P. herbarium</i> + e-waste	2	7.9
	1	34.6
<i>P. herbarium</i> – e-waste	1	13.0

4. Discussion

Metal recovery from the e-waste varied among fungal species and type of metal, with recoveries ranging from 0.15 to 20.59%. *P. sporulosa* demonstrated the greatest percentage of recovery for Cu whereas *P. brasiliensis* had the greatest recoveries of Mn and Co. Despite the differences among the three fungi for specific metals, a general pattern was observed in terms of their recoveries following the order: Cu > Mn > Co > Ni. We note that, because these fungi produce Mn oxides, Cu having the greatest recoveries suggests differences in the mechanisms of metal retention by fungi and biominerals, as discussed below.

4.1. Siderophores, Metal Speciation in Media, and the Mechanism of Dissolution

In media extracts, only Fe was complexed by fungal siderophores in our experiment. The absence of siderophore complexes of Cu, Mn, Co, and Ni, this can be attributed to competition for complexation by Fe despite the $25\text{--}575 \times$ greater concentration of the metal ions relative to Fe in the culture medium. Siderophores are known to preferentially bind Fe with remarkably high stability constants ($K_{\text{stability}} = 10^{25}\text{--}10^{50}$) [34–36], facilitating preferential binding of Fe over divalent transition metals [37]. Fe is required by most microorganisms at 0.05 to 1.8 μM [38,39], and siderophore production is typically increased under iron depleted conditions, with specific siderophores often playing different roles in iron transport. For instance, ferricrocin is known to be an intracellular iron storage compound conserved across many fungal species, whereas coprogen is known to be an extracellular siderophore secreted in response to low iron [35,40,41]. Conversely, when Fe is abundant, siderophore production is typically suppressed, with inhibitory Fe concentrations specific to the organism and the siderophores produced [42,43]. In this study, sufficient Fe supply in the culture medium (4 μM Fe) likely explains the lack of extracellular siderophores produced even before e-waste was introduced. However, it is interesting to note that, despite the high-Fe concentration, greater production of siderophores and greater complexation of Fe occurred with e-waste addition.

Toxic metals alter siderophore-mediated mechanisms for both metal detoxification and nutrient acquisition. For instance, enhanced siderophore production has also been reported in toxic environments [44–46], in conformity with our findings. This appears to be true for siderophores that bind to heavy metals outside the cell and prevent cellular uptake of complexed metals [44]. However, for metals (such as Al) whose toxicity to fungi is intensified by DFAM, a bacterial siderophore, fungal siderophore production decreased with Al toxicity (Illmer and Buttinger, 2006). Interestingly, using the same fungi, Al toxicity was diminished when 10 μM Fe was supplied [47], suggesting that metal toxicity to fungi can be compensated for by nutrient bioavailability, particularly by Fe. It is worth noting that siderophores are known to have several functions beyond iron transport [48], and their cause for increased production in this system was not definitely determined herein.

The presence of recovered metals in their inorganic forms suggest that the fungi had released the e-waste metals via other means not involving chelation by siderophores or other biogenic ligands. Although the physical action of fungi can contribute to weathering [49], we did not observe the growth of fungi into our plates, suggesting a chemical mechanism. Beyond complexation, other chemical mechanisms of fungal bioweathering include acidification and reduction [50]. These strategies both involve the exudation of small organic acids to manipulate the chemistry of the hyphosphere [51]. Although we did not examine small organic acidic exudation in this study, we speculate that the solubilization of metals from e-waste may thus be driven by the exudation of small organics, such as citrate and oxalate [52], that may broadly promote the dissolution of mineral phases [53].

4.2. Fungal-Associated Metal Speciation

Metal solubilized from e-waste may adsorb onto or be taken up by fungi [54], or adsorbed onto Mn oxides [15]. The well-defined Mn-rich particles produced by *P. brasiliensis* (Figure 3) are consistent with the formation of fungal Mn oxide biominerals [55]. Furthermore, Co, whose trivalent form is similar in size to tetravalent Mn, is known to be effectively incorporated into the structure of Mn oxides [56–58]. Although Ni has also been associated with fungal Mn oxides [19], its low recovery may account for its absence in SEM-EDS data. *P. sporulosa*, which had a lesser recovery of Mn, also showed Mn particles but did not show collocated Co, possible due to lesser recoveries.

Interestingly, Cu, which had generally greater percentage recoveries, did not form concentrated deposits on fungi. Although Cu may also associate with Mn oxides [22] or form discrete metallic nanoparticles on fungi [59], our results suggest a diffuse distribution on the fungal body, suggesting adsorption to biomass may be the dominant mechanism of its sequestration [60]. Lesser recoveries and the lack of observed particles associated with *P. herbarium* suggest that sorption may also be the dominant form of metal recovery associated with this fungus in our experiments.

Overall, our findings show the contrasting potential of fungi to recover Mn, Cu, and Co from e-waste that was incorporated directly into the solid fungal growth medium. However, the magnitude of extracted metals in our tests are much lower in comparison to the levels obtained from bioleaching approaches. Bahaloo-Horeh and Mousavi [61] recovered up to 100% Cu, 77% Mn, 64% Co, and 54% Ni from a spent Li-ion cellular phone battery (1%–2% *w/v*) after 8 days of incubation and bioleaching of the e-waste using organic acid-rich (cell-free) medium from *Aspergillus niger* cultures. Similar levels of the metals (94% Cu, 72% Mn, 38% Co and 45% Ni) were also extracted from bioleaching the same e-waste materials and bioleaching solutions after an extended incubation period of 30 days [62]. Heydarian et al. [63] also reported 89.4% Ni and 50.4% Co recovered from Li ion batteries from bioleaching with *Aspergillus thiooxidans* and *A. ferrooxidans* cultures. Bioleaching using cultures of other microorganisms on various types of e-wastes typically ranges from 35 and 99.9% Cu (the most common metal recovered across different types of e-wastes) depending on laboratory parameters controlled such as e-waste particle size and pulp density, leaching pH, temperature, incubation/leaching period, and supplemental C or Fe [9,64].

It is worth mentioning that our experimental approach of supplementing our culture medium with a high-Fe concentration may have decreased the amounts of siderophores produced. Alternatively, if no Fe was added, siderophore production may have increased and complexation may have influenced the speciation of other transition metals. However, under this Fe-free scenario, fungal growth and survival may have been impacted due to the lack of detectable Fe in the e-waste used. Hence, future studies aimed at optimizing metal recovery should consider the optimum Fe supplement required without negatively impacting siderophore production.

5. Conclusions

Our experiment showed the capacity of Mn oxidizing fungi to recover metals derived from e-waste incorporated into a solid medium. Contrary to our hypothesis, metals

were not recovered through complexation with any of the detected siderophores due to preferential siderophore binding with the Fe supplied in the nutrient growth medium, suggesting that reduction and acidification as the main mechanism of dissolution from e-waste. The close association between Mn and Co in discrete particles observed from the SEM images suggests the presence of Mn oxides with *P. brasiliensis*. In contrast, the diffuse distribution of Cu suggests that it is not predominately associated with Mn oxides and thus may bond to fungal assemblages via a different mechanism.

P. brasiliensis recovered the most Mn and Co at 8.45% and 1.75%, respectively, whereas *P. sporulosa* extracted the most Cu at 20.59% *w/w* from e-waste. None of the fungi recovered significant amounts of Ni (0.33%–0.45%). Although the efficiencies of our fungal cultures were lower compared to bioleaching approaches, optimizing fungal growth conditions with the e-waste might increase their e-waste metal recovery in the future. For example, experiments with different media [65], including Fe-depleted media, may change fungal exudation and stimulate solubilization. Furthermore, physical changes to fungal growth, such as growth in liquid media or direct contact between fungi and waste [61,62], may also produce increased recoveries. We also note the need to determine recoveries for other trace metals to reduce the possibility of mobilization of potential toxins during the bioleaching process.

Author Contributions: Conceptualization, O.W.D., O.B. and M.A.C.; methodology, S.A.D., M.A.C., O.B. and O.W.D.; siderophore and metal speciation analysis, O.B.; writing—original draft preparation, S.A.D. and O.B.; writing—review and editing, O.W.D., S.A.D. and O.B.; visualization, O.B. and S.A.D.; supervision, O.W.D.; project administration, O.W.D.; funding acquisition, O.W.D., O.B. and M.A.C. All authors have read and agreed to the published version of the manuscript.

Funding: This research was funded by the Research and Innovation Seed Funding Program (RISF) from the NC State University Office of Research and Innovation (ORI). This work was supported by the USDA National Institute of Food and Agriculture, Hatch projects NC02713 and NC02951. We thank Retriev Technologies, Inc. for providing our sample of battery waste. This work was performed in part at the Analytical Instrumentation Facility (AIF) at North Carolina State University, which is supported by the State of North Carolina and the National Science Foundation (award number ECCS-2025064). The AIF is a member of the North Carolina Research Triangle Nanotechnology Network (RTNN), a site in the National Nanotechnology Coordinated Infrastructure (NNCI). This work was performed in part by the Molecular Education, Technology and Research Innovation Center (METRIC) at NC State University, which is supported by the State of North Carolina. This work was performed in part at the Environmental and Agricultural Testing Service Laboratory (EATS), Department of Crop and Soil Sciences, at North Carolina State University.

Data Availability Statement: The data presented in this study is contained within the article.

Conflicts of Interest: The authors declare no conflicts of interest.

References

1. World Economic Forum and Platform for Accelerating the Circular Economy (PACE). *A New Circular Vision for Electronics: Time for a Global Reboot*; World Economic Forum: Cologne, Switzerland, 2019.
2. Forti, V.; Balde, C.P.; Kuehr, R.; Bel, G. *The Global E-Waste Monitor 2020: Quantities, Flows and the Circular Economy Potential*; United Nations University/United Nations Institute for Training and Research, International Telecommunication Union, and International Solid Waste Association: Bonn, Germany; Geneva, Switzerland; Rotterdam, The Netherlands, 2020.
3. Shittu, O.S.; Williams, I.D.; Shaw, P.J. Global E-waste management: Can WEEE make a difference? A review of e-waste trends, legislation, contemporary issues and future challenges. *Waste Manag.* **2021**, *120*, 549–563. [[CrossRef](#)] [[PubMed](#)]
4. Andeobu, L.; Wibowo, S.; Grandhi, S. An assessment of e-waste generation and environmental management of selected countries in Africa, Europe and North America: A systematic review. *Sci. Total Environ.* **2021**, *792*, 148078. [[CrossRef](#)] [[PubMed](#)]
5. Chauhan, G.; Jadhao, P.R.; Pant, K.K.; Nigam, K.D.P. Novel technologies and conventional processes for recovery of metals from waste electrical and electronic equipment: Challenges & opportunities—A review. *J. Environ. Chem. Eng.* **2018**, *6*, 1288–1304. [[CrossRef](#)]
6. Zhang, K.; Schnoor, J.L.; Zeng, E.Y. E-Waste Recycling: Where Does It Go from Here? *Environ. Sci. Technol.* **2012**, *46*, 10861–10867. [[CrossRef](#)] [[PubMed](#)]
7. Anaya-Garzon, J.; Hubau, A.; Joulian, C.; Guezennec, A.-G. Bioleaching of E-Waste: Influence of Printed Circuit Boards on the Activity of Acidophilic Iron-Oxidizing Bacteria. *Front. Microbiol.* **2021**, *12*, 669738. [[CrossRef](#)]

8. Yaashikaa, P.R.; Priyanka, B.; Senthil Kumar, P.; Karishma, S.; Jeevanantham, S.; Indraganti, S. A review on recent advancements in recovery of valuable and toxic metals from e-waste using bioleaching approach. *Chemosphere* **2022**, *287*, 132230. [[CrossRef](#)]
9. Adetunji, A.I.; Oberholster, P.J.; Erasmus, M. Bioleaching of Metals from E-Waste Using Microorganisms: A Review. *Minerals* **2023**, *13*, 828. [[CrossRef](#)]
10. Meyer, V.; Basenko, E.Y.; Benz, J.P.; Braus, G.H.; Caddick, M.X.; Csukai, M.; de Vries, R.P.; Endy, D.; Frisvad, J.C.; Gunde-Cimerman, N.; et al. Growing a circular economy with fungal biotechnology: A white paper. *Fungal Biol. Biotechnol.* **2020**, *7*, 5. [[CrossRef](#)]
11. Kraemer, S.M.; Butler, A.; Borer, P.; Cervini-Silva, J. Siderophores and the Dissolution of Iron-bearing Minerals in Marine Systems. In *Molecular Geomicrobiology*; Banfield, J.F., Cervini-Silva, J., Nealson, K.H., Eds.; Mineralogical Society of America: Chantilly, VA, USA, 2005; Volume 59, pp. 53–84.
12. Kraemer, S.M.; Crowley, D.E.; Kretzschmar, R. Geochemical aspects of phytosiderophore-promoted iron acquisition by plants. *Adv. Agron.* **2006**, *91*, 1–46. [[CrossRef](#)]
13. Crumbliss, A.L.; Harrington, J.M. Iron Sequestration by small molecules: Thermodynamic and kinetic studies of natural siderophores and synthetic model Compounds. *Adv. Inorg. Chem.* **2009**, *61*, 179–250.
14. Harrington, J.; Duckworth, O.; Haselwandter, K. The fate of siderophores: Antagonistic environmental interactions in exudate-mediated micronutrient uptake. *BioMetals* **2015**, *28*, 461–472. [[CrossRef](#)] [[PubMed](#)]
15. Tebo, B.M.; Bargar, J.R.; Clement, B.G.; Dick, G.J.; Murray, K.J.; Parker, D.L.; Verity, R.; Webb, S.M. Biogenic manganese oxides: Properties and mechanisms of formation. *Annu. Rev. Earth Planet. Sci.* **2004**, *32*, 287–328. [[CrossRef](#)]
16. Goldberg, E.D. Marine Geochemistry 1. Chemical Scavengers of the Sea. *J. Geol.* **1954**, *62*, 249–265. [[CrossRef](#)]
17. Duckworth, O.W.; Bargar, J.R.; Sposito, G. Sorption of ferric iron from ferrioxamine B to synthetic and biogenic layer type manganese oxides. *Geochim. Cosmochim. Acta* **2008**, *72*, 3371–3380. [[CrossRef](#)]
18. Gardner, T.G.; Rivera, N.; Anderws, M.Y.; Santelli, C.; Duckworth, O.W. Diversity and Abundance of Microbial Community in NC Superfund Site Remediation System Biofilm, and Their Role in Mn Oxidation. In Proceedings of the ASA, CSSA and SSSA International Annual Meetings, Minneapolis, MN, USA, 15–18 November 2015.
19. Droz, B.; Dumas, N.; Duckworth, O.W.; Peña, J. A Comparison of the Sorption Reactivity of Bacteriogenic and Mycogenic Mn Oxide Nanoparticles. *Environ. Sci. Technol.* **2015**, *49*, 4200–4208. [[CrossRef](#)] [[PubMed](#)]
20. Duckworth, O.W.; Rivera, N.A.; Gardner, T.G.; Andrews, M.Y.; Santelli, C.M.; Polizzotto, M.L. Morphology, structure, and metal binding mechanisms of biogenic manganese oxides in a superfund site treatment system. *Environ. Sci. Process. Impacts* **2017**, *19*, 50–58. [[CrossRef](#)]
21. Park, Y.; Liu, S.; Gardner, T.; Johnson, D.; Keeler, A.; Ortiz, N.; Rabah, G.; Ford, E. Biohybrid nanofibers containing manganese oxide-forming fungi for heavy metal removal from water. *J. Eng. Fibers Fabr.* **2020**, *15*, 1558925019898954. [[CrossRef](#)]
22. Peña, J.; Kwon, K.D.; Refson, K.; Bargar, J.R.; Sposito, G. Mechanisms of nickel sorption by a bacteriogenic birnessite. *Geochim. Cosmochim. Acta* **2010**, *74*, 3076–3089. [[CrossRef](#)]
23. Andrews, M.Y.; Santelli, C.M.; Duckworth, O.W. Layer plate CAS assay for the quantitation of siderophore production and determination of exudation patterns for fungi. *J. Microbiol. Methods* **2016**, *121*, 41–43. [[CrossRef](#)]
24. Andrews, M.Y.; Santelli, C.M.; Duckworth, O.W. Digital image quantification of siderophores on agar plates. *Data Brief* **2016**, *6*, 890–898. [[CrossRef](#)]
25. Smith, A.W. 6.13 Iron Starvation and Siderophore-Mediated iron Transport. In *Methods in Microbiology*; Williams, P., Ketley, J., Salmond, G., Eds.; Academic Press: Cambridge, MA, USA, 1998; Volume 27, pp. 331–342.
26. Arnow, L.E. Colorimetric Determination of the Components of 3,4-Dihydroxyphenylalaninetyrosine Mixtures. *J. Biol. Chem.* **1937**, *118*, 531–537. [[CrossRef](#)]
27. Baars, O.; Morel, F.M.M.; Perlman, D.H. ChelomEx: Isotope-Assisted Discovery of Metal Chelates in Complex Media Using High-Resolution LC-MS. *Anal. Chem.* **2014**, *86*, 11298–11305. [[CrossRef](#)] [[PubMed](#)]
28. Baars, O.; Perlman, D.H. Small Molecule LC-MS/MS Fragmentation Data Analysis and Application to Siderophore Identification. In *Applications from Engineering with MATLAB Concepts*; Jan, V., Ed.; IntechOpen: Rijeka, Croatia, 2016; Chapter 9.
29. Whitaker, A.H.; Austin, R.E.; Holden, K.L.; Jones, J.L.; Michel, F.M.; Peak, D.; Thompson, A.; Duckworth, O.W. The structure of natural biogenic iron (oxyhydr)oxides formed in circumneutral pH environments. *Geochim. Cosmochim. Acta* **2021**, *308*, 237–255. [[CrossRef](#)] [[PubMed](#)]
30. Keller-Schierlein, W.; Deér, A. Stoffwechselprodukte von Mikroorganismen. 44. Mitteilung. Zur Konstitution von Ferrichrysin und Ferricrocin. *Helv. Chim. Acta* **1963**, *46*, 1907–1920. [[CrossRef](#)]
31. Schwecke, T.; Göttling, K.; Durek, P.; Dueñas, I.; Käufer, N.F.; Zock-Emmenthal, S.; Staub, E.; Neuhofer, T.; Dieckmann, R.; von Döhren, H. Nonribosomal Peptide Synthesis in *Schizosaccharomyces pombe* and the Architectures of Ferrichrome-Type Siderophore Synthetases in Fungi. *ChemBioChem* **2006**, *7*, 612–622. [[CrossRef](#)]
32. Wang, M.; Carver, J.J.; Phelan, V.V.; Sanchez, L.M.; Garg, N.; Peng, Y.; Nguyen, D.D.; Watrous, J.; Kapon, C.A.; Luzzatto-Knaan, T.; et al. Sharing and community curation of mass spectrometry data with Global Natural Products Social Molecular Networking. *Nat. Biotechnol.* **2016**, *34*, 828–837. [[CrossRef](#)]
33. Bertrand, S.; Larcher, G.; Landreau, A.; Richomme, P.; Duval, O.; Bouchara, J.-P. Hydroxamate siderophores of *Scedosporium apiospermum*. *BioMetals* **2009**, *22*, 1019–1029. [[CrossRef](#)]

34. Renshaw, J.C.; Robson, G.D.; Trinci, A.P.J.; Wiebe, M.G.; Livens, F.R.; Collison, D.; Taylor, R.J. Fungal siderophores: Structures, functions and applications. *Mycol. Res.* **2002**, *106*, 1123–1142. [[CrossRef](#)]
35. Winkelmann, G. Ecology of siderophores with special reference to the fungi. *BioMetals* **2007**, *20*, 379–392. [[CrossRef](#)]
36. Hider, R.C.; Kong, X. Chemistry and biology of siderophores. *Nat. Prod. Rep.* **2010**, *27*, 637–657. [[CrossRef](#)]
37. Kraemer, S.; Duckworth, O.; Harrington, J.; Schenkeveld, W.C. Metallophores and Trace Metal Biogeochemistry. *Aquat. Geochem.* **2015**, *21*, 159–195. [[CrossRef](#)]
38. Martínez, J.L.; Delgado-Iribarren, A.; Baquero, F. Mechanisms of iron acquisition and bacterial virulence. *FEMS Microbiol. Rev.* **1990**, *6*, 45–56. [[CrossRef](#)] [[PubMed](#)]
39. Schaible, U.E.; Kaufmann, S.H.E. Iron and microbial infection. *Nat. Rev. Microbiol.* **2004**, *2*, 946–953. [[CrossRef](#)] [[PubMed](#)]
40. Eisendle, M.; Schrettl, M.; Kragl, C.; Müller, D.; Illmer, P.; Haas, H. The Intracellular Siderophore Ferricrocin Is Involved in Iron Storage, Oxidative-Stress Resistance, Germination, and Sexual Development in *Aspergillus nidulans*. *Eukaryot. Cell* **2006**, *5*, 1596–1603. [[CrossRef](#)] [[PubMed](#)]
41. Wallner, A.; Blatzer, M.; Schrettl, M.; Sarg, B.; Lindner, H.; Haas, H. Ferricrocin, a Siderophore Involved in Intra- and Transcellular Iron Distribution in *Aspergillus fumigatus*. *Appl. Environ. Microbiol.* **2009**, *75*, 4194–4196. [[CrossRef](#)] [[PubMed](#)]
42. Eisendle, M.; Oberegger, H.; Buttinger, R.; Illmer, P.; Haas, H. Biosynthesis and uptake of siderophores is controlled by the PacC-mediated ambient-pH Regulatory system in *Aspergillus nidulans*. *Eukaryot. Cell* **2004**, *3*, 561–563. [[CrossRef](#)] [[PubMed](#)]
43. Haas, H. Molecular genetics of fungal siderophore biosynthesis and uptake: The role of siderophores in iron uptake and storage. *Appl. Microbiol. Biotechnol.* **2003**, *62*, 316–330. [[CrossRef](#)]
44. Braud, A.; Hoegy, F.; Jezequel, K.; Lebeau, T.; Schalk, I.J. New insights into the metal specificity of the *Pseudomonas aeruginosa* pyoverdine–iron uptake pathway. *Environ. Microbiol.* **2009**, *11*, 1079–1091. [[CrossRef](#)]
45. Nair, A.; Juwarkar, A.A.; Singh, S.K. Production and Characterization of Siderophores and its Application in Arsenic Removal from Contaminated Soil. *Water Air Soil Pollut.* **2007**, *180*, 199–212. [[CrossRef](#)]
46. Teitzel, G.M.; Geddie, A.; De Long, S.K.; Kirisits, M.J.; Whiteley, M.; Parsek, M.R. Survival and growth in the presence of elevated copper: Transcriptional profiling of copper-stressed *Pseudomonas aeruginosa*. *J. Bacteriol.* **2006**, *188*, 7242–7256. [[CrossRef](#)]
47. Illmer, P.; Buttinger, R. Interactions between iron availability, aluminium toxicity and fungal siderophores. *Biomaterials* **2006**, *19*, 367–377. [[CrossRef](#)]
48. Johnstone, T.C.; Nolan, E.M. Beyond iron: Non-classical biological functions of bacterial siderophores. *Dalton Trans.* **2015**, *44*, 6320–6339. [[CrossRef](#)] [[PubMed](#)]
49. Money, N.P. Biomechanics of Invasive Hyphal Growth. In *Biology of the Fungal Cell*; Howard, R.J., Gow, N.A.R., Eds.; Springer: Berlin/Heidelberg, Germany, 2001; pp. 3–17.
50. Gadd, G.M. Geomycology: Biogeochemical transformations of rocks, minerals, metals and radionuclides by fungi, bioweathering and bioremediation. *Mycol. Res.* **2007**, *111*, 3–49. [[CrossRef](#)] [[PubMed](#)]
51. Andriano, A.; Guggenberger, G.; Kernchen, S.; Mikutta, R.; Sauheitl, L.; Boy, J. Production of Organic Acids by Arbuscular Mycorrhizal Fungi and Their Contribution in the Mobilization of Phosphorus Bound to Iron Oxides. *Front. Plant Sci.* **2021**, *12*, 661842. [[CrossRef](#)] [[PubMed](#)]
52. Gadd, G.M. Fungal Production of Citric and Oxalic Acid: Importance in Metal Speciation, Physiology and Biogeochemical Processes. In *Advances in Microbial Physiology*; Poole, R.K., Ed.; Academic Press: Cambridge, MA, USA, 1999; Volume 41, pp. 47–92.
53. Martin, S.T. Precipitation and dissolution of iron and manganese oxides. In *Environmental Catalysis*; Grassian, V.H., Ed.; Marcel-Dekker, CRC Press: Boca Raton, FL, USA, 2005; pp. 61–81.
54. Gadd, G.M. Interactions of fungi with toxic metals. *New Phytol.* **1993**, *124*, 25–60. [[CrossRef](#)]
55. Santelli, C.M.; Webb, S.M.; Dohnalkova, A.C.; Hansel, C.M. Diversity of Mn oxides produced by Mn(II)-oxidizing fungi. *Geochim. Cosmochim. Acta* **2011**, *75*, 2762–2776. [[CrossRef](#)]
56. Burns, R.G. The uptake of cobalt into ferromanganese nodules, soils, and synthetic manganese (IV) oxides. *Geochim. Cosmochim. Acta* **1976**, *40*, 95–102. [[CrossRef](#)]
57. Murray, J.W. The interaction of cobalt with hydrous manganese dioxide. *Geochim. Cosmochim. Acta* **1975**, *39*, 635–647. [[CrossRef](#)]
58. Simanova, A.A.; Peña, J. Time-Resolved Investigation of Cobalt Oxidation by Mn(III)-Rich δ -MnO₂ Using Quick X-ray Absorption Spectroscopy. *Environ. Sci. Technol.* **2015**, *49*, 10867–10876. [[CrossRef](#)]
59. Manceau, A.; Nagy, K.L.; Marcus, M.A.; Lanson, M.; Geoffroy, N.; Jacquet, T.; Kirpichtchikova, T. Formation of metallic copper nanoparticles at the soil-root interface. *Environ. Sci. Technol.* **2008**, *42*, 1766–1772. [[CrossRef](#)]
60. Verma, A.; Shalu, Singh, A.; Bishnoi, N.R.; Gupta, A. Biosorption of Cu (II) using free and immobilized biomass of *Penicillium citrinum*. *Ecol. Eng.* **2013**, *61*, 486–490. [[CrossRef](#)]
61. Bahaloo-Horeh, N.; Mousavi, S.M. Enhanced recovery of valuable metals from spent lithium-ion batteries through optimization of organic acids produced by *Aspergillus niger*. *Waste Manag.* **2017**, *60*, 666–679. [[CrossRef](#)] [[PubMed](#)]
62. Bahaloo-Horeh, N.; Mousavi, S.M.; Baniasadi, M. Use of adapted metal tolerant *Aspergillus niger* to enhance bioleaching efficiency of valuable metals from spent lithium-ion mobile phone batteries. *J. Clean. Prod.* **2018**, *197*, 1546–1557. [[CrossRef](#)]
63. Heydarian, A.; Mousavi, S.M.; Vakilchap, F.; Baniasadi, M. Application of a mixed culture of adapted acidophilic bacteria in two-step bioleaching of spent lithium-ion laptop batteries. *J. Power Sources* **2018**, *378*, 19–30. [[CrossRef](#)]

64. Desmarais, M.; Pirade, F.; Zhang, J.; Rene, E.R. Biohydrometallurgical processes for the recovery of precious and base metals from waste electrical and electronic equipments: Current trends and perspectives. *Bioresour. Technol. Rep.* **2020**, *11*, 100526. [[CrossRef](#)]
65. Power, D.A.; Zimbro, M.J. *Difco & BBL Manual: Manual of Microbiological Culture Media*; Difco Laboratories, Division of Becton Dickinson and Co.: Sparks, MD, USA, 2003.

Disclaimer/Publisher's Note: The statements, opinions and data contained in all publications are solely those of the individual author(s) and contributor(s) and not of MDPI and/or the editor(s). MDPI and/or the editor(s) disclaim responsibility for any injury to people or property resulting from any ideas, methods, instructions or products referred to in the content.